Nanotrap Grafted Anionic MOF for Superior Uranium Extraction from Seawater

Yogeshwar D. More,[‡,a] Samraj Mollick,[‡,a,b] Satyam Saurabh,[a] Sahel Fajal,[a] Michele Tricarico,[b] Subhajit Dutta,[a] Mandar M. Shirolkar,[c] Writakshi Mandal,[a] Jin-Chong Tan,[b] and Sujit K. Ghosh*[a,d]*

[a] Department of Chemistry, Indian Institute of Science Education and Research, Dr. Homi Bhabha Road, Pashan, Pune 411008, India. Phone: +91 20 2590 8076.
E-mail: sghosh@iiserpune.ac.in
[b] Multifunctional Materials & Composites (MMC) Laboratory, Department of Engineering Science, University of Oxford, Parks Road, Oxford OX1 3PJ, United Kingdom.
E-mail: jin-chong.tan@eng.ox.ac.uk
[c] Symbiosis Center for Nanoscience and Nanotechnology (SCNN), Symbiosis International (Deemed University) (SIU), Lavale, Pune 412115, India.
[d] Centre for Water Research (CWR), Indian Institute of Science Education and Research, Dr. Homi Bhabha Road, Pashan, Pune 411008, India.

Keywords: Uranium extraction, anionic MOF, trace amount, energy, fast kinetics, record capacity, selectivity, recyclability, mechanistic insight

---

Abstract: On-demand uranium extraction from seawater (UES) could mitigate growing sustainable energy needs, while high salinity and low concentration hinder its recovery. We demonstrated a novel anionic metal-organic framework (iMOF-1A) adorned with rare Lewis basic pyrazinic sites as uranyl-specific nanotrap serving as robust ion exchange material for selective uranium extraction, rendering its intrinsic ionic characteristics to minimize leaching. Ionic adsorbents sequestrated 99.8 % of the uranium in just 120 mins (from 20,000 ppb to 24 ppb) and adsorbed extraordinarily large amounts of 1336.8 mg g^{-1} and 625.6 mg g^{-1} from uranium-spiked deionized water and artificial seawater, respectively, with very high distribution coefficient, $K_d^U \geq 0.97 \times 10^6$ mL g^{-1}. The material offers a very high enrichment index of ~5754 and it achieves the UES standard of 6.0 mg g^{-1} in just 16 days, and harvests 9.42 mg g^{-1} in 30 days from natural uncontaminated seawater. Isothermal titration calorimetry (ITC) studies quantified thermodynamic parameters, previously uncharted in uranium sorption experiments. Infrared nearfield nanospectroscopy (nano-FTIR) and tip-force microscopy (TFM) enabled chemical and mechanical elucidation of host-guest interaction at atomic level

in sub-micron crystals revealing extant capture events throughout the crystal rather than surface solely. Comprehensive experimentally guided computational studies revealed ultrahigh-selectivity for uranium from seawater, marking mechanistic insight.

1. Introduction

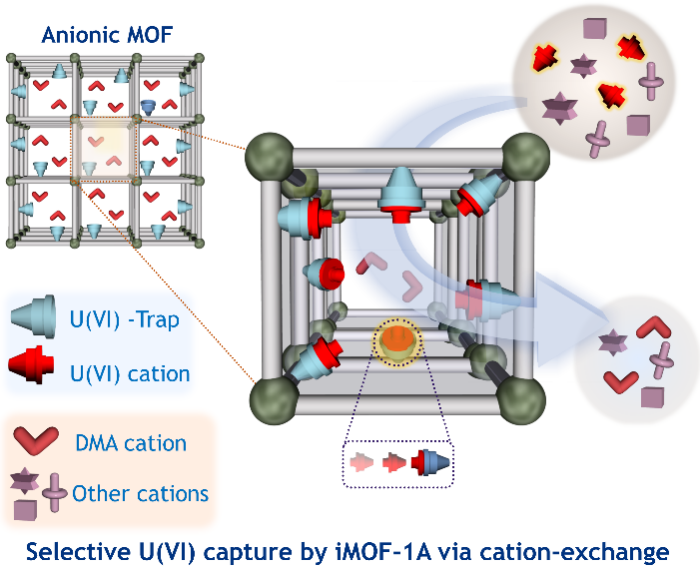

Scheme 1. A schematic representation of nanotrap grafted cation exchangeable MOF selectively capturing Uranyl ions from a mixture of other interfering cations.

We are in the age of soaring global energy demand and witnessing intense turmoil that is shaking our globe. Energy consumption varies according to a multitude of socioeconomic factors such as urbanization, incremental population, industrialization, extent of socio-economic development, and furtherance in technology. Following the depletion of traditional energy sources, long-term sustainable energy supply has become one of the most serious concerns that mankind is confronting.[1] Accounting various ecological issues that are related to burning of fossil fuels including pollution, global warming, and biodiversity disasters, the necessity for alternative energy sources has immense significance both in science and technology.[2] Amongst the mature technologies, nuclear energy is one of the most desirable low-carbon choices due to its low contribution towards greenhouse gases.[1] The enormous growth of nuclear activities linked to uranium mining , refining, and recuperation is vital for the reliable supply of sustainable energy, as uranium is a pivotal component in nuclear reactors. However, it's a matter of concern that the there is an incremental shortage of geological reserves of uranium ores, which will be drained in less than a century or even sooner by the current consumption rate of global usage.[3] In this regard, there are roughly 4.5 billion tonnes of

uranium in the ocean, rendering it a conceivably colossal resource to support nuclear production for millennia.[4,5] Uranium recuperation from seawater demands state-of-the-art materials research and is thought to be one of the seven most demanded chemical separations that, at whatever point improved, would bring revolutionary global benefits.[6] Although significant efforts have been put into the development of varieties of new adsorbents aimed for uranium extraction from seawater (UES).[3,7-11,12] However, on a laboratory scale, their performances are frequently limited, and the majority of them suffer from extremely low adsorption kinetics, limited uptake capacity, and poor selectivity thereby making them undesirable candidates for efficient uranium extraction. Therefore, the development of new durable adsorbents that satisfy the stringent commercial standards set by the economic evolution of UES is much needed to fulfill the critical demand for sustainable energy supply.[14]

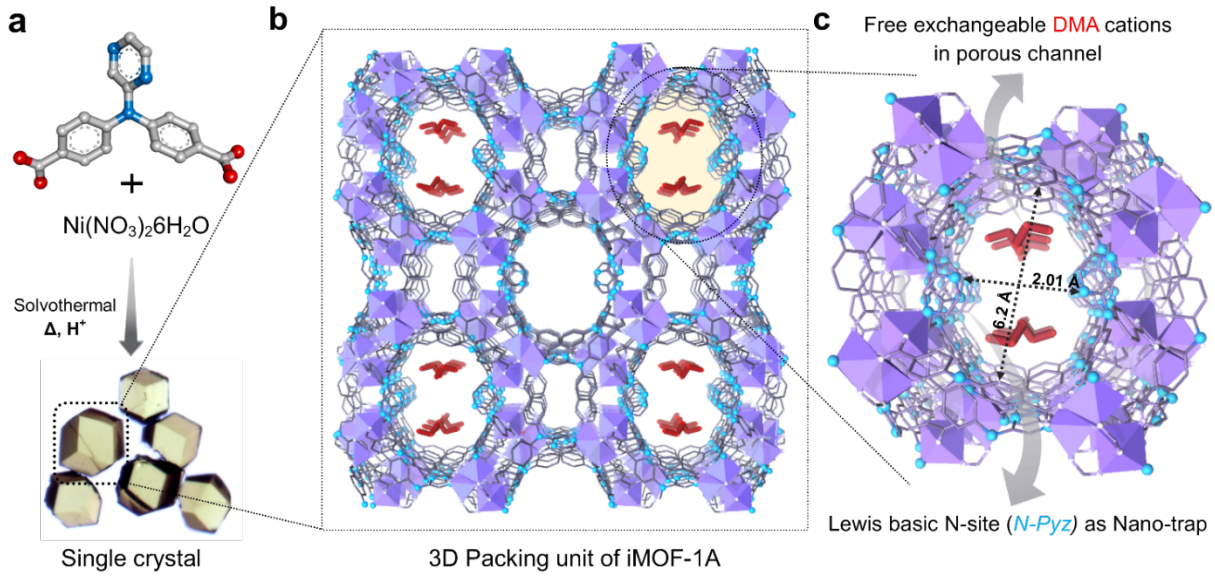

Figure 1. a) Representation of the synthetic protocol leading to iMOF-1A, by varying the uncoordinated anions within its pores; b) Perspective view of iMOF-1A revealing its bi-porous nature with two types of Ultramicroporous channels sustaining the framework; c) Orderly arrangement of DMA cations within pore; (colour codes: grey—C, cyan-blue—N, white—O, purple—Ni, guest—scarlet red (DMA cations), Solvent molecules and H atoms are omitted for clarity).

Within reticular chemistry, metal-organic frameworks (MOFs) are champion materials formed by coordination between metal centers (clusters or metal ions) and organic struts.[15,16] Ionic MOFs (i-MOFs) are potentially the most significant MOF-based host matrix manifestations accounting for residual charge (negative or positive) that can be recurrently

exchanged with more appropriate ions, and thereby are capable of imparting a desirable functional properties. Anionic MOFs (iMOF-A), a subclass of ionic MOFs, have been considered a class of multifunctional materials given their plethoric propositions in the fields of selective capture, gas storage, drug delivery, catalysis, photonic applications, nanogenerators and many more.[17-20] The habitation of charged species within the frameworks results in specified interactions that can be efficiently utilized as ion-exchange sorbents for sequestration of cationic guests. The leaching probability of the trapped cationic guests is also avoided as the entrapped cation is an integral part of the framework as a charge−balancing ion. Additionally ionic features with easily accessible Lewis basic sites could offer additional benefits due to the selective binding affinity of certain analytes inside the frameworks (Scheme 1).[21,22] Recently MOF−based adsorption and electrocatalytic extraction techniques have become the frontrunner for the selective capture of multifarious pollutants, including radioactive species, due to their unprecedented potential.[23,24] While tremendous efforts are being devoted to the detailed realization of chemical and structural features that influence the adsorption process, the complete thermodynamics of MOF−analyte interactions occurring in aqueous media has left mostly unexplored, even though it is crucial for designing the next−generation sorbents.

Herein, we sought to exploit an anionic MOF for the efficient recovery of uranium through both ion-exchange and interaction processes. iMOF-1A, being a hydrolytically stable anionic framework, hold the potential to be a forerunner in this regime in view of the freely lying dimethyl ammonium (DMA) cations that can be easily substituted to afford the multifaceted applications. The anionic adsorbent (iMOF-1A) captures 99.8 % uranium in only 120 min (20000 ppb to 24 ppb) and delivers a very high distribution coefficient $K_d^U \geq 0.97$ X 10^6 mL g^{-1}, representing a strong affinity for uranium. An iMOF-1A exhibited very high uranium adsorption capacity of 1336.8 mg g^{-1} from water compared to other reported MOFs. The material efficiently reduced the trace amounts of uranium levels in a range of water sources, including potable water, lake water, river water, and artificial seawater, to less than the United States (U.S.) Environmental Protection Agency (EPA) drinking water limits. The anionic adsorbent can extract more than half of uranium from natural seawater (7.1 gallons), and it recovers 9.38 mg g^{-1} (batch 1) uranium within 30 days from natural seawater with an exceptional enrichment index of ~5754, also additional sets of reproduced experiments reveal average uranium recovery of ~9.42 mg g^{-1} (for N = 3, Table S8) in 30 days. The ITC experiments provide the detailed quantification of the thermodynamics of adsorption processes in aqueous media, which was unexplored in the literature for the uranium adsorption process. Furthermore, the nano-FTIR and TFM studies demonstrated that the sequestration process is

associated with both ion exchange and supramolecular interactions throughout the single crystals of iMOF-1A. Moreover, combined experimental and computational studies revealed that excellent selectivity and high uranium capacity are attributed to the formation of chelation with the densely decorated Lewis basic N-sites of the framework.

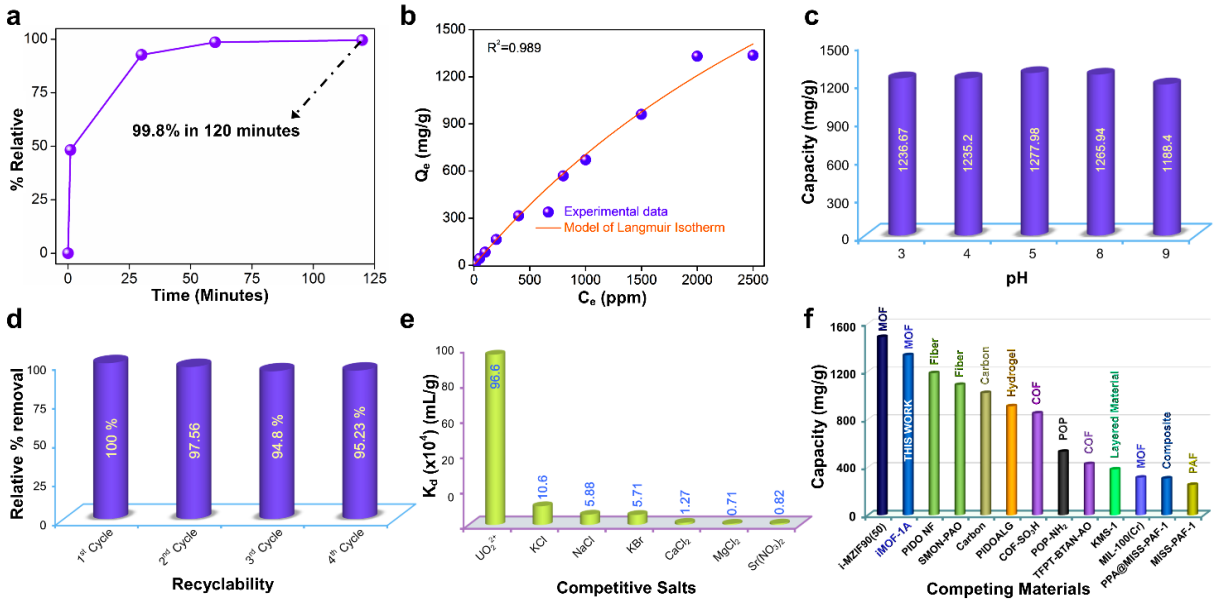

Figure 2. Uranium capture from various uranium-spiked water systems by iMOF-1A. (a) Kinetics of uranium removal efficiency from spiked water samples spiked with 20,000 ppb uranium at V/m = 2250 mL g^{-1}. (b) Langmuir isotherms. (c) pH dependent adsorption capacity tests. (d) Recyclability test. (e) Distribution coefficient, K_d value of iMOF-1A for different meddling cations. (f) Comparison of uranium adsorption capacities from uranium-spiked water comprising various reported excellent adsorbents (Table S3).

2. Result and Discussion

The iMOF-1A was synthesized on a gram scale (Figure S1–S7) by the solvothermal method, where a mixture of ligand (LH_2=4,4'-(pyrazin-2-ylazanediyl)dibenzoic acid) and $Ni(NO_3)_2.6H_2O$ was heated at 120 °C in a programmable oven for 48 h (Figure S1–S6 and Scheme S1–S2, see the experimental section for more details). Single-crystal X-ray diffraction revealed that the compound crystallized in the centrosymmetric cubic (*I*23) space groups. The co-ordination environment for iMOF-1A realized to be {[Ni_3L_3(μ-O)][2·DMA]}; where L = 4,4'-(pyrazin-2-ylazanediyl)dibenzoate, which constitutes free dimethyl ammonium ($(CH_3)_2NH_2^+$ i.e. DMA) cation and free pyrazinic nitrogen sites (Pyz-N) in the framework (Figure 1). The exchangeable free DMA cations are present in an orderly pattern within the channels of the 3D pore, while free Lewis basic nitrogen sites are densely anchored within the

pore (Figure S8). The bulk phase crystallinity and purity were confirmed from the powder X-ray diffraction (PXRD) patterns (Figure S9). Thermogravimetric analysis (TGA) showed there is a pertinent loss of free guest molecules up to about 220 °C (Figure S10). Variable temperature powder X-ray diffraction (VT-PXRD) patterns collected upon heating the compound at higher temperatures confirmed the sustained structural integrity of the compound up to ~400 °C (Figure S11b). The chemical stability of the materials was examined by immersing the material in different chemical environments, besides its persistence in natural seawater (Figure S11a–S11c, Movie S1). Unaltered PXRD patterns confirmed the retention of structural integrity in water and other solvents spanning several days (Figure S11a). Further, the crystal of iMOF-1A was kept immersed in a wide range of pH solutions and the similarity in PXRD patterns confirmed the exceptional stability over a broad pH range (Figure S11a–S11c).

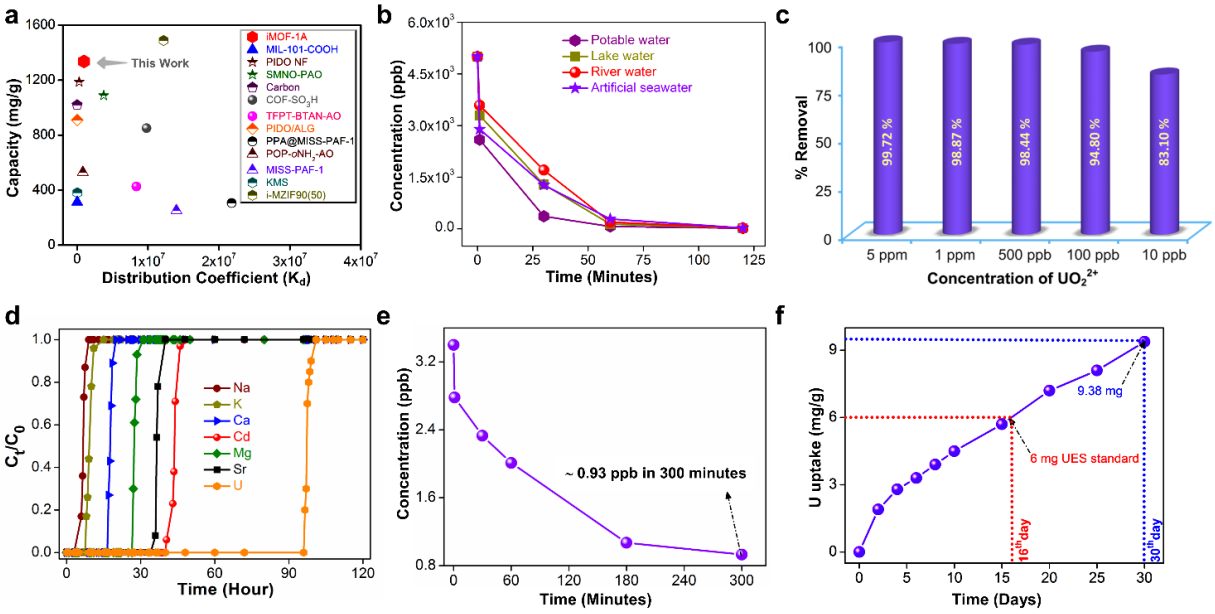

Figure 3. Uranium capture from spiked seawater as well as nonspiked natural seawater by iMOF-1A. (a) Comparison of uranium adsorption capacities against distribution coefficient for various excellent adsorbents from water. (b) The kinetics of uranium removal efficiency from various water samples spiked with 5000 ppb uranium at V/m = 2666.7 mL g^{-1}. (c) Removal % of U from various trace amounts of U spiked artificial seawater by iMOF-1A at V/m = 1000 mL g^{-1}. (d) Breakthrough experiments of a mixed solution composed of 3 ppm uranium and 3 ppm other competitive metal cations in water through iMOF-1A packed bed. (e) Removal % of U from natural nonspiked seawater (i.e. natural seawater). (f) The adsorption performance for uranyl ions during 30 days of close contact with natural seawater (uranyl ion concentration of ~3.4 ppb) meeting UES standards.

After thorough elucidation of iMOF-1A stability through accelerated stability tests (Figure S12 A–B), we sought to harness the virtue of ionic functionality imparted by the chemically robust anionic framework bearing ordered Pyz-N and tertiary amine sites for the investigation of uranium capture studies.[25,27] As an underlying screening test, after dipping iMOF-1A crystals in uranium-spiked water for a few hours (Movie S1), the colour of the solution went through slight decoloration and the green crystals turned to yellow (Figure S13–S14). Enthused by these findings, we systematically carried out the uranium sorption experiments and monitored them through the inductively coupled plasma mass spectroscopy (ICP-MS). The saturation capacity in 20 ppm of uranium-spiked water can be accomplished only within 120 min, with negligible leaching of iMOF-1A which shows acute contrast to other adsorbents taking a longer adsorption time (Figure 2a, Figure S15–S16, and Table S1). The experimental data fitted well with the pseudo-second-order kinetics, implying the sorption of uranyl cation onto iMOF-1A is a due to chemisorption (Figure S17). The experimental isotherm data fit well with the Langmuir model, confirming monolayer chemical adsorption of uranyl ions on ionic adsorbents (Figure 2b and Figure S17–S19). The material adsorbed 1336.8 mg g^{-1} uranium from the water sample under scrutiny, as assessed from the isotherm data. It is noteworthy that this obtained capacity value is among the highest in the MOF domain and undisputedly comparable to the other reported excellent uranium adsorbents (Figure 2f and Tables S2, S3).[3,11,26]

The materials also adsorbed uranium from a wide range of pH solutions, which indeed confirmed that the iMOF-1A is an exceptional candidate material for being a suitable material for uranium recuperation from seawater (Figure 2c, Figure S20). The ionic adsorbents are easily recycled up to several consecutive cycles without much loss of their original efficacy, demonstrating their huge potential for extracting uranium from seawater (Figure 2d, Figure S21 and Table S4).

High salinity in natural seawater critically influences the adsorption of trace levels of uranium.[28] Thereby, high and selective capture of trace amounts of uranium from a huge combination of other competing cations in the same solution is absolutely critical for UES.[11,13,26] To estimate the affinity of uranium towards the framework and its functionalities, the distribution coefficient (K_d) has been calculated (Figure 2e–2f, Figure 3a and Figure S22, Table S5). Materials exhibiting a K_d value > 10^4 mL g^{-1} are being considered as decent adsorbent for uranium extraction.[29] The calculated K_d value for iMOF-1A is notably ~0.97 x 10^6 mL g^{-1}, which is two orders of magnitude higher and it is comparable with the excellent

adsorbents reported in existing literature (Figure 3a and Table S3, Table S5).[23,30] The exceptionally high K_d value indicates the strong interaction between the framework and uranium ions. The materials are also capable of efficiently reducing uranium from a variety of water systems, such as potable water, lake water, river water, and artificial seawater to less than 30 ppb, which is the U.S. Environmental Protection Agency's designated limit for hazardous waste and drinking water standards (Figure 3b and Figure S23–S27, Table S6, Table S7).[31] Adsorption of several interfering metal ions from spiked natural seawater was also performed, study reveals greater adsorption capacity for uranium in comparison with other metal cations reflecting the remarkable selectivity towards uranium compared to other metal ions (Figure S28).

While pursuing seawater uranium extraction, a trace quantity of uranium extraction was also performed from artificial seawater (Figure S29). It was found that the iMOF-1A efficiently reduces the trace amount of uranium out of artificial seawater, confirming the conceivable capability of this material for uranium recuperation from the seawater (Figure 3c). Further, breakthrough experiments were performed by utilizing the precisely weighed desolvated phase of iMOF-1A to estimate the real-world practical applicability of this material for uranium capture from seawater. The complete breakthrough for all cations was detected within 21 hours, in contrast, uranyl cations conceded 67 hours to pass through the iMOF-1A bed (Figure 3d, Figure S30). The remarkable selectivity towards uranyl cations contrasted with other competing cations is attributed to strong coordinative interactions observed between uranyl ions and the free Lewis basic nitrogen sites (Pyz-N) serving as nanopocket-trap in the form of anchoring's protruded from the pore surface of the ionic MOF i.e. iMOF-1A. All these remarkable experimental reveal that the anionic adsorbents could be leveraged as a novel adsorbent for specified uranium recuperation from seawater.

Finally, the uranium extraction by iMOF-1A was performed on natural seawater, using the samples collected from the Arabian Sea, Mumbai, India.[32] The iMOF-1A reduced over half of the uranium content (3.4 ppb to 1.63 ppb) and adsorbed 9.38 mg g^{-1} (batch 1) of uranium within just 30 days (Figure 3e–3f and Table S7), also its reproducibility results are highly consistent and averaging at 9.42 mg g^{-1} (Table S8). It is noteworthy to mention that this value is the comparable to other phenomenal adsorbents within a short period reported thus far (Table S7). The calculated enrichment index of this material is ~5754, representing an excellent adsorbent for uranium extraction from seawater. It is worth noting that the process of extracting uranium using these materials may incur higher costs compared to the conventional uranium extraction process due to the involvement of nickel metal ions. Hence, we posit that the use of

MOFs composed of Zn, Al, Fe, or Ti/Zr would be more appropriate for practical applications owing to their comparatively affordable cost, large-scale production, and ecological compatibility [33, 34]. This aspect is currently being taken into account in the laboratory.

For detailed exploration of the thermodynamic parameters behind the adsorption processes transpiring in iMOF-1A within aqueous media, isothermal titration calorimetry (ITC) experiments (Figure 4, Figure S31–S35) were performed on competitive cations.[35,36] ITC measurements offer the direct quantification of entropy, enthalpy, and Gibb's free energy changes that are underpinning the adsorption processes, and can be quantified in a single experiment (Figure S34–S35, Table S9). Model divalent and monovalent competing cations, Ca^{2+} and Na^{+} were selected for the study besides UO_2^{2+} cations for the ITC experiments (Figure 4a–c). The ITC investigation reveals that the adsorption process is thermodynamically favoured as signified by the negative change in Gibbs free energy and that the adsorption phenomenon depicted here proceeds via exothermic processes (Figure 4a–f). We observed that UO_2^{2+} adsorption is entropically more favoured compared to other competitive model cations for the adsorption events (Figure 4d–f).

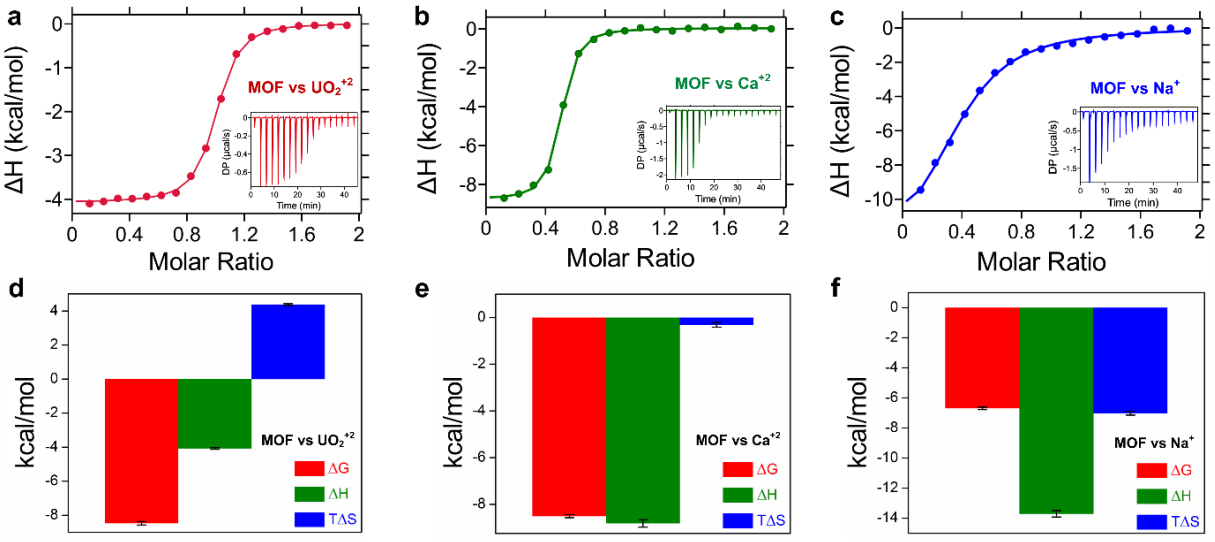

Figure 4. ITC thermograms resulting from injections of (a) UO_2^{2+} salts, (b) Ca^{2+} salts, and (c) Na^{+} salts. The inset depicts the magnitude of the exothermic peaks. The magnitude of thermodynamic parameters of (d) UO_2^{2+} salts, (e) Ca^{2+} salts, and (f) Na^{+} salts; demonstrating uranium chemisorption and entropy relevance in comparison to other cations.

Additionally, from the ITC experiments, it was confirmed that uranium interacted with the Lewis basic nitrogen decorated sites of the frameworks i.e., Pyz-N. Stoichiometric

coefficients obtained from ITC investigations suggest nearly full occupancy for the UO_2^{2+} cation (~1), whereas Ca^{2+} and Na^{+} show partial occupancies, supporting the aforementioned observations (N sites, Table S9).[37] It is worth noting that this study underlines a maiden attempt in the literature addressing comprehensive investigation of the thermodynamic features of uranium adsorption (capture) in aqueous systems comprising top competing cations, and entails the potential to be a routine integrative tool for future sorption and separation studies in solutions.

To gain a detailed insight into the uranium and MOF interaction processes, several experimental and computational studies were carried out (Figure5–6, and Figure S36–S58 and Tables S10–S11). Raman spectra revealed the existence of characteristic peaks for uranium in the spectrum after the MOF was exchanged with uranium (Figure S43). FTIR spectra showed that the characteristics of vibrational spectra red-shifted from 932 cm^{-1} to 912 cm^{-1} following

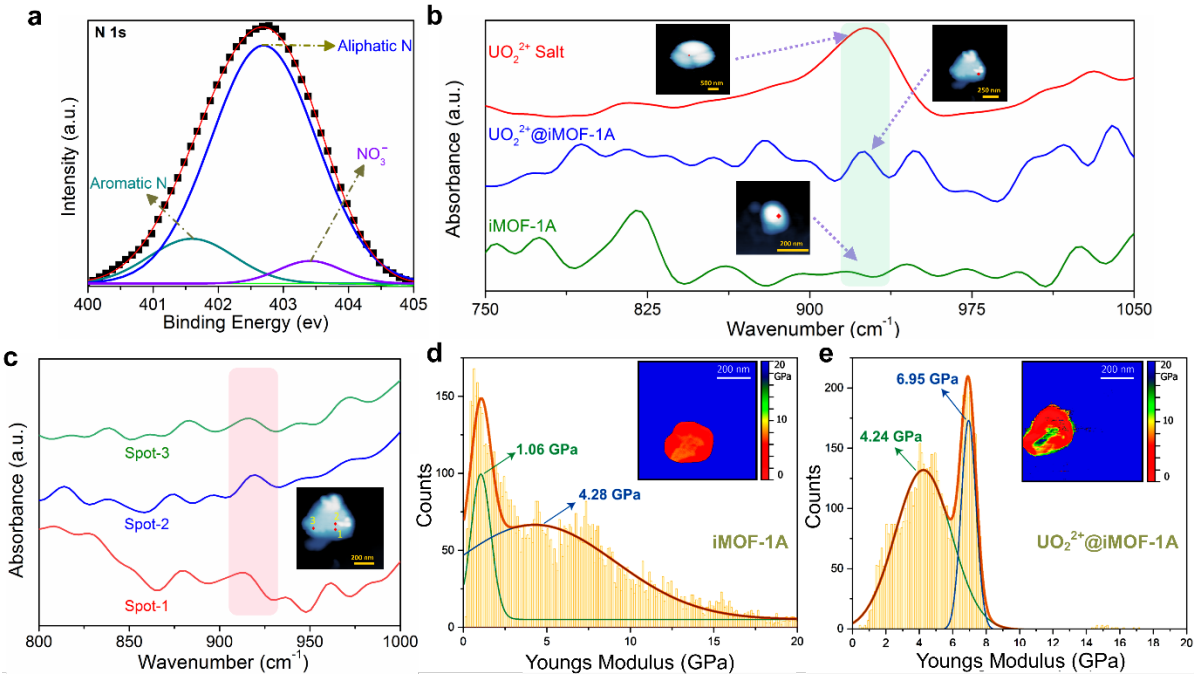

Figure 5. Uranium capture in iMOF-1A single crystals; a) Magnified XPS spectra of N 1s for UO_2^{2+}@iMOF-1A; b) Nano-FTIR spectra of iMOF-1A, UO_2^{2+}@iMOF-1A and UO_2^{2+} salt, inset: nanoscopic spots corresponding to a probe size of ~20 nm; c) Local probing spots of UO_2^{2+}@iMOF-1A; d) TFM for iMOF-1A; e) TFM quantification plots for UO_2^{2+}@iMOF-1A, TFM reconstructions corresponding to different pressure points showing local stiffnesses of a single crystal.; insets: the Young's modulus map.

the adsorption on the surface of iMOF-1A (Figure S44). The peak shifting towards a lower vibration frequency confirmed that there is a strong interaction between the surface of the adsorbent and cationic uranyl ions. The direct evidence of interaction between framework and uranyl ions was further examined by XPS measurement (Figure 5a, Figure S45–S49). The XPS survey spectra exhibit binding energy peaks for U 4f shifted to a lower binding energy region demonstrating firm interactions of uranyl ions with iMOF-1A. The magnified characteristics N 1s peak revealed that uranyl cation strongly interacted with the Pyz-N within the framework (Figure 5a).

The nano-FTIR spectroscopy was employed to probe the host-guest interactions at the single-crystal level with a spatial resolution that beats the diffraction limit of light (Figure 5b, 5c).[38,39] This technique combines scattering-type scanning near-field optical microscopy (s-SNOM) with infrared nanospectroscopy to measure vibrational spectra reflecting local complex characteristics of individual sub-micron crystals where, notably even a single-crystal X-ray diffraction is inaccessible. Rendering to local complex character of the framework, its symmetry is disrupted at a probing depth of 20 nm along the grain boundary of the iMOF-1A crystals that resulted in slightly broadened and additional peaks in nano-FTIR spectra as compared to the far-field ATR-FTIR spectra. Large single crystals are first broken down into tiny fragments to reveal the interior, and then suitable sub-micron crystals are chosen randomly for nano-FTIR local probing. Each spectrum was generated by averaging over 12 independent measurements with an integration time of 14 sec and was then normalised to the silicon substrate spectrum.

The appearance of a characteristic vibrational band of UO_2^{2+} in the UO_2^{2+}@iMOF-1A at 926 cm^{-1} confirms the presence of UO_2^{2+} in the MOF host-framework by exchanging with DMA cations (Figure 5b). The presence of a distinctive UO_2^{2+} vibrational band in different local positions of randomly selected MOF single crystal fragments are evidencing the exchange process had occurred throughout the bulk crystals. The characteristic peak for UO_2^{2+} is occasionally redshifted within the same crystal fragments, indicating that sequestration is driven by both ion exchange and supramolecular interaction processes (Figure 5c). Mechanical characteristics may also be determined using the s-SNOM setup, deploying contact mode rather than tapping mode, via technique termed as tip force microscopy (TFM).[40,41] The TFM approach supplies us with the local mechanical properties of individual nanocrystals in the form of a Young's modulus map generated from a sample surface's stiffness data. The Young's modulus maps on the crystals are shown in the inset figures in the picture, where the red region represents the TFM probing zone and the blue region represents the silicon substrate (Figure

5d, 5e). The bimodal distribution of the Young's modulus is visible throughout the pure MOF single crystals (Figure 5d). However, after the uranium exchanging process, a much higher stiffness value of ~7 Gigapascal (GPa) appeared in addition to the ~4.2 GPa throughout the crystals (Figure 5e). The appearance of a new modulus throughout the crystals shows that both; ion exchange and supramolecular interaction processes are involved in the uranium capture experiments.

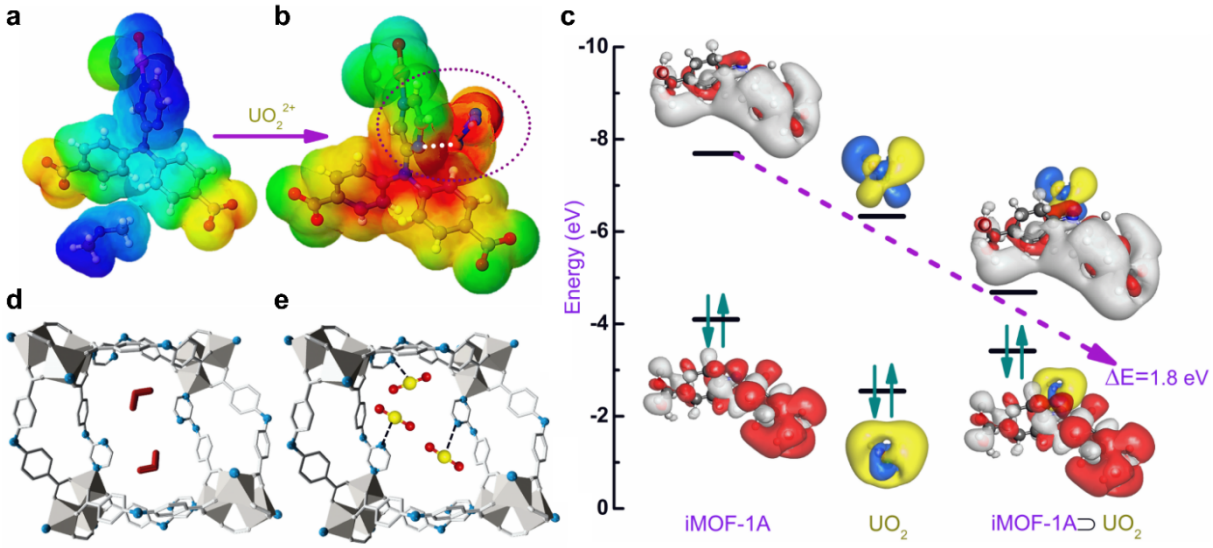

Figure 6. a) ESP of asymmetric unit of iMOF-1A and b) ESP of iMOF-1A unit after UO_2 interactions. c) Distribution of HOMO–LUMO in an iMOF-1A, UO_2^{2+} and after interaction between iMOF-1A and UO_2^{2+}. DFT-optimized guest-interaction sites in iMOF-1A including; d) exchangeable DMA cations and e) UO_2^{2+}, highlights the N···UO_2^{2+} interaction between the framework Pyz-N atoms and UO_2^{2+} molecules.

Herein, the observed experimental results were further corroborated by density functional theory (DFT) simulations (Figure 6, Figure S54-S57). Figure 6a shows ESP of the asymmetric unit of iMOF-1A and Figure 6b shows the ESP of the iMOF-1A unit after UO_2^{2+} interactions. It is interesting to note that the ESP of iMOF-1A drastically changes after UO_2^{2+} interactions and the coordination of DMA cation with iMOF-1A disappears. The study shows that UO_2^{2+} selectively interacts with aromatic nitrogen's (Pyz-N) of iMOF-1A. We further determined HOMO-LUMO interactions between iMOF-1A and UO_2^{2+} to extract changes in the energy level. This quantum mechanical information is essential for estimating the collective electronic interactions between iMOF-1A and UO_2^{2+}. The HOMO governs the electron donation ability of a molecule, while LUMO dictates its electron acceptance ability. Therefore,

the active sites between the molecules are responsible for the physicochemical interactions. The Figure 6c reveals the distribution of HOMO–LUMO within iMOF-1A, UO_2^{2+} and after interaction between iMOF-1A with UO_2^{2+}. It can be seen that initially before UO_2^{2+} interactions, HOMO and LUMO of iMOF-1A are having a separation of ~4 eV, while the separation between HOMO–LUMO of UO_2^{2+} is around ~2.4 eV; interestingly, the interaction between iMOF-1A and UO_2^{2+} decreased the HOMO–LUMO gap to ~1.8 eV. The theoretical findings were realized by employing frontier molecular orbital theory as well as Koopman's theorem. As seen, the LUMO of UO_2^{2+} lies between the valance band and conduction band of iMOF-1A. This allows electron transfer from the iMOF-1A HOMO to the UO_2^{2+} LUMO., which further decreases the HOMO–LUMO energy gap of the combined system. To gain additional mechanistic insights into the extant interaction process occurring between iMOF-1A and UO_2^{2+}, we considered the single subunit of iMOF-1A (Figure 6d). Since a single subunit of iMOF-1A bears two DMA cations, the cation exchange process renders framework interaction that allows both of the DMA cations to be selectively replaced by a single UO_2^{2+}, per subunit; thereby UO_2^{2+} further interacts with the aromatic Lewis basic nitrogen site (Pyz-N) of iMOF-1A achieving a stabilized form within the iMOF-1A scaffold. It is important to note that the interaction of UO_2^{2+} with iMOF-1A is selective and remains unaltered in the presence of other competing cations, viz., NaCl, KCl, $SrCl_2$, Mg $(NO_3)_2$, $CdCl_2$ (Figure S54-S58). Uranium exists in seatwater as a triscarbonatouranyl anion.[42] The anionic form of uranium adsorbed on the MOF is primarily due to interactions between the pyrazine's nitrogen (Pyz-N) and the U center of the triscarbonatouranyl anion.[43] This interaction mechanism drives uranium uptake, resulting in a considerably lower capacity of 9.38 mg g^{-1} compared to spiked seawater (625.6 mg g^{-1}) where uranium is present as uranyl ion (UO_2^{2+}). Adsorption in spiked seawater systems is a cooperative effect of both ion exchange and interaction processes.

3. Conclusion

We have successfully demonstrated uranium extraction by a highly stable and novel anionic MOF (iMOF-1A) through both the ion exchange and interaction processes. The framework is capable of the efficient capturing of trace amounts of uranium in a wide range of water systems, including artificial seawater. The ionic adsorbent exhibited ultrafast capture kinetics with a remarkably high enrichment index (5754) and high sorption capacity derived dually from both; uranium spiked water and natural seawater, i.e., 1336.8 mg g^{-1} and 9.38 mg g^{-1}, respectively, which are among the highest values reported in the domain of MOFs. The nano-FTIR and TFM studies supported the notion of U capture that occurs throughout the MOF

crystals, confirming that both ion exchange processes and supramolecular interactions are involved in the uranium sequestration studies. Observations are further supported by coherently detailed computational studies. The current findings might pave the way for new avenues aimed at efficient uranium extraction blended by crucially significant experimental evaluation and molecular level analysis, which will help trigger the development of novel anionic MOFs or similar materials, besides the inclusion of crucial corroboratory experimental tools for the remediation of high-risk environmental pollutants.

Associated Content

CCDC 2208426 contains the supplementary crystallographic data for this paper. These data can be obtained free of charge from The Cambridge Crystallographic Data Centre via www.ccdc.cam.ac.uk/data_request/cif

Supporting Information

Supporting Information is available from the Wiley Online Library or from the author. Additional experimental details and figures including structures, ESI-TOF-MS, PXRD patterns, FESEM images, elemental mapping, ITC data and plots, nano-FITR images, TFM plots, N_2 sorption isotherms, TGA curves, NMR spectra, ICP data plot, RAMAN and IR plots, photographs, capture studies, removal % values, recyclability test results (PDF), Supporting Movie S1 (ZIP) and CIF files. This material is available free of charge via the Internet.

Author Information

Corresponding Author

*[a,d] Prof. Sujit K. Ghosh (S.K.G.), Department of Chemistry, Indian Institute of Science Education and Research, Dr. Homi Bhabha Road, Pashan, Pune 411008, India. Phone: +91 20 2590 8076; E-mail: sghosh@iiserpune.ac.in

*[b] Prof. Jin-Chong Tan (J.C.T.), Multifunctional Materials & Composites (MMC) Laboratory, Department of Engineering Science, University of Oxford, Parks Road, Oxford OX1 3PJ, United Kingdom.; E-mail: jin-chong.tan@eng.ox.ac.uk

Author Contributions

The Y. D. M. and S. M. conceptualised and planned the research. Y. D. M., S. M., S. S. and S. F. conducted experiments and analysed data. Y.D.M. and S.M. wrote the paper. Y.D.M., S.D., and S. F. shaped all the graphical works. M. M. S. performed the theoretical studies. Under the

direction of J.C.T., M.T. and S. M. carried out the TFM and nano-FTIR measurements, respectively. S.K.G. supervised the research and the completion of the manuscript. J.C.T. supported the nano-FTIR, TFM measurements besides manuscript correction. All authors have approved the final version of the manuscript.

‡These authors contributed equally.

Funding Sources

S.K.G. acknowledges funding supports from DST-SERB project (CRG/2019/00906), S.M., M.T., and J.C.T. are grateful to the ERC Consolidator Grant (PROMOFS grant agreement 771575) and the EPSRC (EP/R511742/1) for funding the research.

Notes

The authors declare no competing interests.

Acknowledgement

Y.M. and S.D. are thankful to IISER Pune for fellowship. S.M. and S.F. acknowledges UGC (India) and INSPIRE (India) for fellowship respectively. S.K.G. acknowledges funding supports from DST-SERB project (CRG/2019/00906), IISER Pune. S.M., M.T., and J.C.T. are grateful to the ERC Consolidator Grant (PROMOFS grant agreement 771575) and the EPSRC (EP/R511742/1) for funding the research. MMS thank SIU for technical support. Y.M. is also thankful to Bhavin Uttekar and IISER Pune Microscopy facility for measurements.

Received: ((will be filled in by the editorial staff))

Revised: ((will be filled in by the editorial staff))

Published online: ((will be filled in by the editorial staff))

References

[1] S. Chu, A. Majumdar, *Nature* **2012**, *488*, 294.

[2] Q. Schiermeier, J. Tollefson, T. Scully, A. Witze, O. Morton, *Nature* **2008**, *454*, 816.

[3] N. Tang, J. Liang, C. Niu, H. Wang, Y. Luo, W. Xing, S. Ye, C. Liang, H. Guo, J. Guo, Y. Zhang, G. Zeng, *J. Mater. Chem. A* **2020**, *8*, 7588.

[4] S. Zhang, H. Li, S. Wang, *Chem* **2020**, *6*, 1504.

[5] C. W. Abney, R. T. Mayes, T. Saito, S. Dai, *Chem. Rev.* **2017**, *117*, 13935.

[6] D. S. Sholl, R. P. Lively, *Nature* **2016**, *532*, 435.

[7] M. J. Manos, M. G. Kanatzidis, *Chem. Sci.* **2016**, *7*, 4804.

[8] T. Zheng, Z. Yang, D. Gui, Z. Liu, X. Wang, X. Dai, S. Liu, L. Zhang, Y. Gao, L. Chen, D. Sheng, Y. Wang, J. Diwu, J. Wang, R. Zhou, Z. Chai, T. E. Albrecht-Schmitt, S. Wang, *Nat Commun.* **2017**, *8*, 15369.

[9] X. Yang, J. Li, J. Liu, Y. Tian, B. Li, K. Cao, S. Liu, M. Hou, S. Li, L. Ma, *J. Mater. Chem. A* **2013**, *2*, 1550.

[10] J. Li, X. Dai, L. Zhu, C. Xu, D. Zhang, M. A. Silver, P. Li, L. Chen, Y. Li, D. Zuo, H. Zhang, C. Xiao, J. Chen, J. Diwu, O. K. Farha, T. E. Albrecht-Schmitt, Z. Chai, S. Wang, *Nat Commun.* **2018**, *9*, 3007.

[11] S. Mollick, S. Saurabh, Y. D. More, S. Fajal, M. M. Shirolkar, W. Mandal, S. K. Ghosh, *Energy & Environ. Sci.* **2022**, *15*, 3462.

[12] C. W. Abney, R. T. Mayes, M. Piechowicz, Z. Lin, V. S. Bryantsev, G. M. Veith, S. Dai, W. Lin, *Energy Environ. Sci.* **2016**, *9*, 448.

[13] Z. Wang, Q. Meng, R. Ma, Z. Wang, Y. Yang, H. Sha, X. Ma, X. Ruan, X. Zou, Y. Yuan, G. Zhu, *Chem* **2020**, *6*, 1683.

[14] C. Xiao, M. A. Silver, S. Wang, *Dalton Trans.* **2017**, *46*, 16381.

[15] Hong-Cai "Joe" Zhou, S. Kitagawa, *Chem. Soc. Rev.* **2014**, *43*, 5415.

[16] G. Maurin, C. Serre, A. Cooper, G. Férey, *Chem. Soc. Rev.* **2017**, *46*, 3104.

[17] Y. D. More, S. Saurabh, S. Mollick, S. K. Singh, S. Dutta, S. Fajal, A. Prathamshetti, M. M. Shirolkar, S. Panchal, M. Wable, S. Ogale, S. K. Ghosh, *Adv. Mater. Interfaces* **2022**, 2201713.

[18] A. B. Spore, N. L. Rosi, *CrystEngComm* **2017**, *19*, 5417.

[19] P. Li, N. A. Vermeulen, X. Gong, C. D. Malliakas, J. F. Stoddart, J. T. Hupp, O. K. Farha, *Angew. Chem., Int. Ed. Engl.* **2016**, *55*, 10358.

[20] F. Zarekarizi, S. Beheshti, A. Morsali, *Inorg. Chem. Commun.* **2018**, *97*, 144.

[21] H. Li, F. Zhai, D. Gui, X. Wang, C. Wu, D. Zhang, X. Dai, H. Deng, X. Su, J. Diwu, Z. Lin, Z. Chai, S. Wang, *Appl. Catal. B.* **2019**, *254*, 47.

[22] J. Yu, Y. Cui, H. Xu, Y. Yang, Z. Wang, B. Chen, G. Qian, *Nat Commun.* **2013**, *4*, 2719.

[23] Q. Sun, B. Aguila, J. Perman, A. S. Ivanov, V. S. Bryantsev, L. D. Earl, C. W. Abney, L. Wojtas, S. Ma, *Nat Commun.* **2018**, *9*, 1644.

[24] L. Zhang, N. Pu, B. Yu, G. Ye, J. Chen, S. Xu, S. Ma, *ACS Appl. Mater. Interfaces* **2020**, *12*, 3688.

[25] X. H. Xiong, Z. W. Yu, L. L. Gong, Y. Tao, Z. Gao, L. Wang, W. H. Yin, L. X. Yang, F. Luo, *Adv. Sci.* **2019**, *6*, 1900547.

[26] D. Wang, J. Song, J. Wen, Y. Yuan, Z. Liu, S. Lin, H. Wang, H. Wang, S. Zhao, X. Zhao, M. Fang, M. Lei, B. Li, N. Wang, X. Wang, H. Wu, *Adv. Energy Mater.* **2018**, *8*, 1802607.

[27] S. Ma, L. Huang, L. Ma, Y. Shim, S. M. Islam, P. Wang, L.-D. Zhao, S. Wang, G. Sun, X. Yang, M. G. Kanatzidis, *J. Am. Chem. Soc.* **2015**, *137*, 3670.

[28] Y. Yuan, S. Zhao, J. Wen, D. Wang, X. Guo, L. Xu, X. Wang, N. Wang, *Adv. Funct. Mater.* **2019**, *29*, 1805380.

[29] W.-R. Cui, C.-R. Zhang, W. Jiang, F.-F. Li, R.-P. Liang, J. Liu, J.-D. Qiu, *Nat Commun.* **2020**, *11*, 436.

[30] Y. Yuan, Q. Meng, M. Faheem, Y. Yang, Z. Li, Z. Wang, D. Deng, F. Sun, H. He, Y. Huang, H. Sha, G. Zhu, *ACS Cent. Sci.* **2019**, *5*, 1432.

[31] Q. Sun, B. Aguila, L. D. Earl, C. W. Abney, L. Wojtas, P. K. Thallapally, S. Ma, *Adv. Mater.* **2018**, *30*, 1705479.

[32] R. Rengarajan, M. M. Sarin, S. Krishnaswami, *Oceanol. Acta* **2003**, *26*, 687.

[33] J.-B. Lin, T. T. T. Nguyen, R. Vaidhyanathan, J. Burner, J. M. Taylor, H. Durekova, F. Akhtar, R. K. Mah, O. Ghaffari-Nik, S. Marx, N. Fylstra, S. S. Iremonger, K. W. Dawson, P. Sarkar, P. Hovington, A. Rajendran, T. K. Woo, G. K. H. Shimizu, *Science* **2021**, *374*, 1464.

[34] S. Dai, C. Simms, I. Dovgaliuk, G. Patriarche, A. Tissot, T. N. Parac-Vogt, C. Serre, Chem. Mat. **2021**, *33*, 7057.

[35] S. Kato, R. J. Drout, O. K. Farha, *Cell Reports Physical Science* **2020**, *1*, 100006.

[36] R. J. Drout, S. Kato, H. Chen, F. A. Son, K. Otake, T. Islamoglu, R. Q. Snurr, O. K. Farha, *J. Am. Chem. Soc.* **2020**, *142*, 12357.

[37] W. B. Turnbull, A. H. Daranas, *J. Am. Chem. Soc.* **2003**, *125*, 14859.

[38] A. F. Möslein, M. Gutiérrez, B. Cohen, J.-C. Tan, *Nano Lett.* **2020**, *20*, 7446.

[39] A. F. Möslein, J.-C. Tan, *J. Phys. Chem. Lett.* **2022**, *13*, 2838.

[40] M. Tricarico, J.-C. Tan, *Mater. Today Nano* **2022**, *17*, 100166.

[41] A. F. Möslein, L. Donà, B. Civalleri, J.-C. Tan, *ACS Appl. Nano Mater.* **2022**, *5*, 6398.

[42] A. T. Saito, S. Brown, S. Chatterjee, J. Kim, C. Tsouris, R. T. Mayes, L.-J. Kuo, G. Gill, Y. Oyola, C. J. Janke, S. Dai, *J. Mater. Chem. A* **2014**, *2*, 14674.

[43] A J. Sessler, P. Melfi, G. Pantos, *Coordination Chemistry Reviews* **2006**, *250*, 816.

The table of contents (TOC)

A novel anionic metal-organic framework (iMOF-1A) adorned with a rare Lewis basic pyrazinic nitrogen (Pyz-N) site acting as a uranyl-specific Nanotrap that functions as an effective and recyclable adsorbent is reported herein. The resulting ionic adsorbent has been deployed in uranium sequestration with state-of-the-art mechanistic understanding, delivering epitome performance by rapidly and selectively capturing remarkable amounts of uranium from seawater and range of water bodies.

Yogeshwar D. More,[‡,a] Samraj Mollick,[‡,a,b] Satyam Saurabh,[a] Sahel Fajal,[a] Michele Tricarico,[b] Subhajit Dutta,[a] Mandar M. Shirolkar,[c] Writakshi Mandal,[a] Jin-Chong Tan,[b] and Sujit K. Ghosh*[a,d]*

Nanotrap Grafted in Anionic MOF for Superior Uranium Extraction from Seawater